Available online at www.sciencedirect.com
SCIENCE DIRECT
Journal of Solid State Chemistry 179 (2006) 1119–1128
JOURNAL OF SOLID STATE CHEMISTRY
www.elsevier.com/locate/jssc

Nanocrystalline CaF_2 particles obtained by high-energy ball milling

G. Scholz[a,*], I. Dörfel[b], D. Heidemann[a], M. Feist[a], R. Stösser[a]

[a]*Institut für Chemie, Humboldt-Universität zu Berlin, Brook-Taylor-Street 2, D-12489 Berlin, Germany*
[b]*Bundesanstalt für Materialforschung und -prüfung, 12200 Berlin, Germany*

Received 13 December 2005; accepted 23 December 2005
Available online 7 February 2006

Abstract

Structural changes in mechanically treated CaF_2 powders have been studied by X-ray diffraction, transmission electron microscopy, thermal analysis, ^{19}F and ^{1}H MAS Nuclear Magnetic Resonance and Electron Paramagnetic Resonance methods.

Applying the same methods, the results could be compared with those of mechanochemically synthesized CaF_2 samples, prepared for the first time in this study by high-energy ball milling. The applied methods indicate that the mechanically treated samples become, under the applied conditions, *nanocrystalline*. Unexpectedly, the mechanochemically synthesized samples show the same effects, i.e., nanocrystalline samples were formed. In contrast to many oxide compounds, a weak amorphization takes place only after a strong mechanical impact, and essentially in grain boundaries of spherical particles. Observed effects after the application of mechanical impact like broadening of XRD reflections, broadening of ^{19}F resonances, or the decreasing ability for $H^{\bullet}$ trapping at ambient temperature, are mainly due to decreasing particle sizes as well as very small structural changes in the bulk of the particles. Surprisingly, the spin relaxation of both nuclear spins (^{19}F) and electron spins ($H^{\bullet}$) appears to be the most sensitive tool for the investigation of mechanically and chemically induced changes indicating the increasing surface to bulk ratio with increasing mechanical impact.

Keywords: Mechanochemistry; XRD; EPR; MAS NMR; TEM

1. Introduction

The fast developing field of mechanochemistry of inorganic solids is currently restricted to mainly oxide systems and alloying processes [1–5]. In addition, "soft mechanochemical synthesis" using hydroxides, hydrates or carbonates as starting materials is of increasing importance at the formation of oxide solids with properties opening new fields of application (e.g., nanoceramics, bioceramics, catalysts) [6].

Although nanostructured high-surface area metal fluorides are of increasing importance for different application fields like heterogeneous catalysis, thin films or glasses [7–10], only few papers exist on mechanical activation and/or mechanochemical reactions of solid fluorides. This is due to the peculiar properties of solid fluorides: e.g., the high ionic bonding character, their comparably low hardness accompanied by some elasticity and the high moisture sensitivity.

First publications concern the mechanochemical synthesis of $AZnF_3$ compounds ($A = K$, Na, NH_4) with perovskite structure [11], the synthesis of complex fluorides ARF_4 ($A = Li$, Na, K; $R =$ rare-earth elements) [12], as well as the mechanochemical synthesis of lanthanum oxofluoride LaOF using LaF_3 and La_2O_3 [13]. All reactions mentioned were performed in a planetary mill under access of air. The products were investigated exclusively by X-ray diffraction (XRD) [13]. Further studies were published on milling of PbF_2 and NH_4F with SnF_2 to examine the influence of grain sizes on the ion conductivity [14–16]. More recently, mechanochemical reactions of alkali acid bifluorides (MHF_2) with alkali halides (MX) were studied by XRD and IR spectroscopy [17]. The influence of AlF_3 and ZnF_2 particles on the phase transition from γ-Al_2O_3 to α-Al_2O_3 was studied by XRD and transmission electron microscopy (TEM) measurements [18]. The electrochemical activity of BiF_3 could be

*Corresponding author.
E-mail address: Gudrun.Scholz@rz-hu-berlin.de (G. Scholz).

0022-4596/$ - see front matter © 2006 Elsevier Inc. All rights reserved.
doi:10.1016/j.jssc.2005.12.035

enabled in BiF_3/C nanocomposites prepared by high-energy ball milling [19].

So far, only few papers exist on the application of magnetic resonance methods on mechanically activated solids and especially activated solid fluorides (see, e.g., Refs. [20,21]).

In the present study, CaF_2 was chosen as model substance to follow changes in the matrix under the influence of a mechanical impact for several reasons:

CaF_2 has a well-known simple structure. Although no phase transition to another modification is known, calculations suggest possible, but less stable structures as alternative possibilities on the energy landscape [22,23]. In analogy to other fluoride systems the tendency to structural relaxation of the CaF_2 matrix is accompanied by the formation of limited crystalline particles. It is a peculiarity of the chosen matrix here that atomic hydrogen $H^{\bullet}$, which is known to be stabilized in CaF_2 single crystals [24–27] and powders [28–30] could also be used as a very sensitive and additional spin probe in the unmilled and mechanically treated powder samples after γ-irradiation.

Moreover, the choice of CaF_2 as model substance for the present study is supported by its increasing use as a component in the starting mixture of the mechanochemical synthesis of nanostructured fluorapatite [31]. Also, CaF_2 represents one of the classical materials for dosimetric measurements by its ability to trap holes and electrons. Exploring the ability of $H^{\bullet}$ trapping, it is just this property which will be used here to characterize very small structural changes in the bulk of the nanoparticles.

Two different ways are attempted in this paper to generate nanocrystalline powders of CaF_2: (i) milling of a commercially available crystalline CaF_2 powder, selected by purity from different offers and (ii) a mechanochemical synthesis of CaF_2 starting from $CaCO_3$ and NH_4F according to:

$$CaCO_3 + 2NH_4F \rightarrow CaF_2 + 2NH_3 + H_2O + CO_2.$$

Therefore, it is the intention of this contribution to follow changes of the local structure of nuclear (^{19}F, ^{1}H) and electron ($H^{\bullet}$) spin probes as consequence of the mechanical activation and mechanochemical synthesis by ^{19}F and ^{1}H MAS NMR and EPR spectroscopies in relation to findings obtained by TEM, XRD, and thermal analysis (TA).

Based on the methods mentioned above the new findings of the present contribution concern the formation of nanocrystalline CaF_2 applying both preparation ways mentioned above. Of special interest is the fact that a differentiation between mechanically treated commercial CaF_2 and mechanochemically synthesized CaF_2 powders is only possible with the help of spin probes and their relaxation behaviour.

2. Experimental section

The commercially available powder sample of CaF_2 (Riedel–de Haen) was selected as starting material for milling experiments presented in this paper. This sample contains only traces of Mn^{2+} ions.

This calcium fluoride powder was milled in a commercial planetary mill "Pulverisette 7" (Fritsch, Germany) under access of air applying milling times of 4, 8, and 16 h. Each syalon vial was used with five syalon balls (m_{balls}: 14.8 g; m_{CaF_2}: 2g) and a rotational speed of 600 rpm (rpm: rotations per minute). Additionally, a double impact (ten syalon balls per vial, $m_{balls} = 29.8$ g) was realized for milling times of 4 and 16 h, respectively.

In addition, the mechanochemical synthesis of CaF_2 beginning with $CaCO_3$ and NH_4F was performed using the same planetary mill (input:molar ratio: 1:2 according to the equation, total mass: 1.74 g; milling intensity: 500 rpm; milling time: 5 and 10 h).

High-resolution XRD patterns were recorded with the XRD 3003 TT equipment (Seifert, Germany) for all samples at room temperature (Cu$K\alpha$-radiation; $5^{\circ} \leqslant 2\Theta \leqslant 90^{\circ}$; step scan: 0.05°, step time: 3 s). The working principle of the milling apparatus together with the fixed milling regime guaranteed the reproducibility as repeated experiments in combination with XRD and NMR measurements showed.

The unmilled CaF_2 powder, the two 16 h milled CaF_2 samples (milled with five balls and 10 balls, respectively) and the mechanochemically synthesized samples were studied using TG-DTA measurements in a Netzsch STA 409C thermobalance (heating rate: 10 K/min under N_2 up to 800 °C).

TEM studies were performed with a 200 kV CM20 microscope and a 400 kV JEOL 4000FX microscope. Bright field images, electron diffraction investigations and EDX examinations were combined for the characterization of the samples. The TEM-samples were prepared by depositing few droplets of a suspension of the powders in alcohol on a carbon coated copper grid.

^{19}F and ^{1}H MAS NMR spectra were recorded on a Bruker AVANCE 400 spectrometer ($\nu_{19F} = 376.4$ MHz; $\nu_{1H} = 400.2$ MHz) using a 2.5 mm double-bearing magic angle spinning (MAS) probe (Bruker Biospin) allowing spinning frequencies up to 35 kHz.

^{19}F MAS NMR spectra were recorded with a $\pi/2$ pulse duration of $p1 = 2\,\mu$s, a spectrum width of 400 kHz and a recycling delay between 30 and 600 s corresponding to the respective T_1 time. The isotropic chemical shifts δ_{iso} of ^{19}F resonances are given below with respect to the $CFCl_3$ standard. Spin lattice relaxation times T_1 of ^{19}F were determined with the inversion recovery method [32].

^{1}H MAS NMR spectra were measured with a sweep width of 200 kHz, an excitation pulse lengths of 2.2 μs. Due to the low proton content of the studied samples and a background signal of the probe of comparable intensity the exact determination of the ^{1}H spin lattice relaxation time using the inversion recovery method was not possible. Therefore, a recycling delay of 60 s was used avoiding saturation effects.

For the $\pi/2$ pulse experiments, existent background signals of both ^{19}F and ^{1}H could be completely suppressed with the application of a phase-cycled depth pulse sequence according to Cory and Ritchey [33], especially designed for each spin probe.

The solid state NMR spectra of both $I = 1/2$ nuclei were handled using the Bruker XWIN-NMR software. Simulations of the ^{19}F and ^{1}H NMR spectra were performed with the DMFIT-software [34].

X-band (9.3 GHz) EPR measurements were performed at 293, 77 and 4.2 K with the spectrometer ERS 300 (ZWG/Magnettech GmbH, Germany). Low-temperature measurements (4.2 K) were performed with a flow-cryostat Heli-Tran (APD Cryogenics, USA). Modulation frequencies of 100 kHz (298 K) and 1 kHz (4.2 K) were applied to study the $H^{\bullet}$ signals after γ-irradiation.

3. Results

3.1. X-ray diffraction

CaF_2 belongs to the well-known fluoride compounds possessing a high symmetric cubic structure. It crystallizes in the space group $Fm\bar{3}m$. A scheme of the fluorite structure is given in Fig. 1a. The unit cell consists of a face-centred cube of Ca^{2+} ions, the F^- ions are centred in the octants of this cube. Every Ca^{2+} ion is surrounded by 8 F^- ions and every F^- ion again by 4 Ca^{2+} ions (Fig. 1a). The corresponding ^{19}F MAS NMR spectrum (central line) is shown in Fig. 1b. In the context of this paper (vide infra) it is interesting to note that solid solutions of the composition $CaF_{2-x}H_x$ ($0 < x \leqslant 1.24$) exist [35]. X-ray and neutron diffraction studies indicated a structure with a statistical substitution of fluoride ions by hydride ions in the unit cell [35]. Consequently, the X-ray powder diffractograms of CaF_2 and $CaF_{2-x}H_x$ cannot be distinguished.

Two selected X-ray diffractograms of (i) the unmilled CaF_2 and (ii) the sample milled for 16 h in the planetary mill are shown in Fig. 2 with the development of the (0 2 2) reflections given as inset. The reflections are characterized by a distinct and continuous broadening with increasing milling time. As expected, they are accompanied by a decrease of intensity. The largest effect on the intensity could be registered in going from 0 to 4 h milling. On the other hand, the double impact (use of 10 balls instead of five balls additionally applied at 4 and 16 h milling time) results only in a small increase of line width regarding the respective other sample. The ratio of the amplitudes of the first two intensive reflections (A_{111}/A_{022}) is reversed comparing the unmilled ($A_{111}/A_{022} = 0.91$) and 16 h milled ($A_{111}/A_{022} = 1.15$) samples (see Fig. 2).

It is important to note that neither additional reflections nor an enlargement of the background could be observed as result of mechanical milling of the commercial sample. The latter should be indicative of a certain amorphous proportion in the samples.

Mean grain sizes of 332 nm (unmilled sample) and 60 nm (16 h milled sample) were determined applying the BGMN program [36].

The positions of the XRD reflections of the mechanochemically synthesized CaF_2 unambiguously demonstrate that CaF_2 could successfully be produced by milling the educts $CaCO_3$ and NH_4F. The width of the reflections are identical to those of the sample milled for 16 h (see Fig. 3).

An XRD measurement of the milled samples performed after annealing in the thermobalance unambiguously indicated the structural perfection of the matrices (see Fig. 4). All reflections became as narrow as in the starting material and even the amplitude ratio of the two intensive reflections ($A_{111}/A_{022} = 0.72$) was nearly rebuilt. These facts imply the presence of only small structural disturbances in the nanoparticles and of only small amounts of amorphous materials.

3.2. DTA

The only important difference between the milled commercial samples is the mass loss at heating of up to 1.83% in the sample treated the strongest. The mass loss is

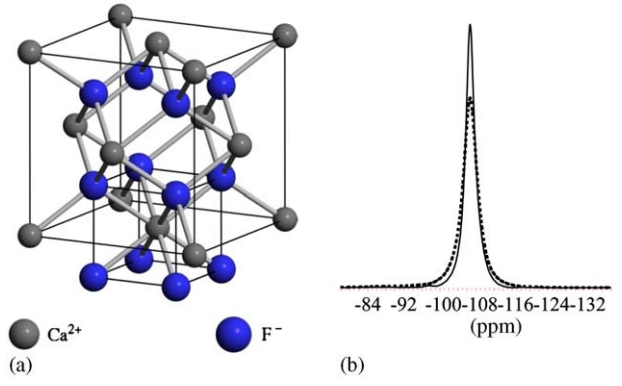

Fig. 1. (a) Detail of the structure of CaF_2 [51] (space group: $Fm\bar{3}m$; lattice constant: $a = 5.463$ Å; R_{F-F} (neighboured) = 2.709 Å, R_{F-F} (diagonal) = 4.709 Å). (b) ^{19}F MAS NMR spectra (central line) of unmilled CaF_2 (___) and 16 h (5 balls) milled CaF_2 (…) (2.5 mm rotor, $\nu_{rot} = 30$ kHz).

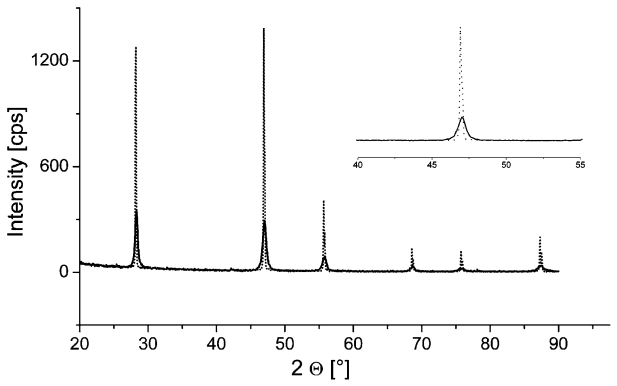

Fig. 2. X-ray powder diffractograms of unmilled CaF_2 (….) and CaF_2 milled for 16 h, 10 balls (___). Inset: enlargement of the (0 2 2) reflections of the two samples.

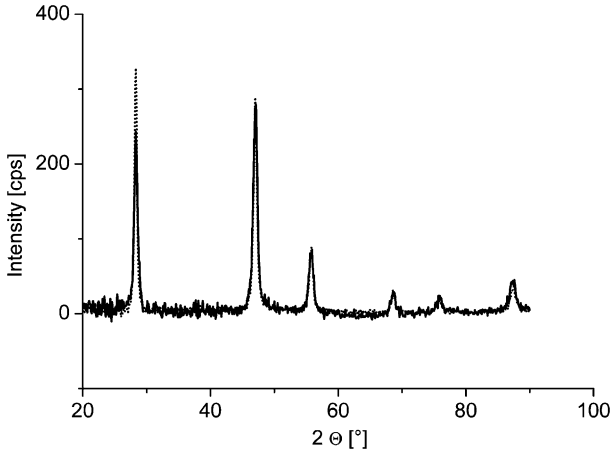

Fig. 3. X-ray powder diffractograms of mechanochemically synthesized CaF_2 (10 h milling) (___) and commercial CaF_2 milled for 16 h, 10 balls (…).

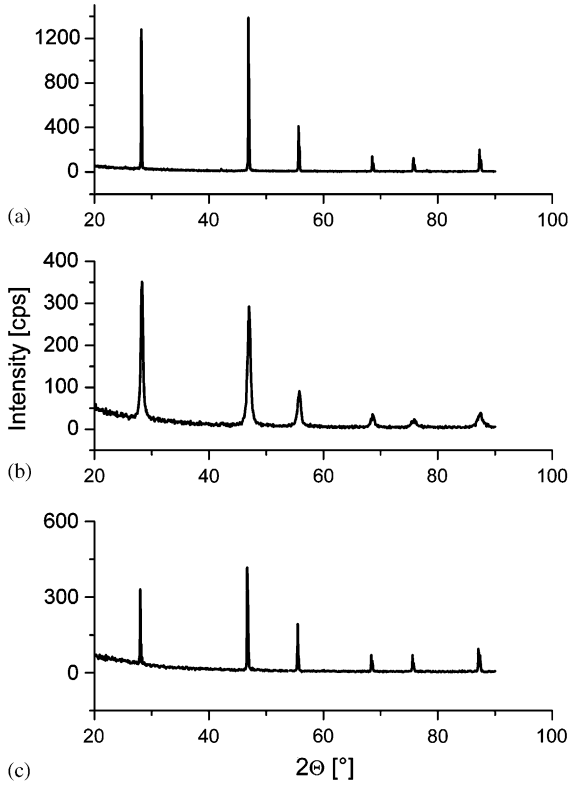

Fig. 4. X-ray powder diffractograms of unmilled CaF_2 (a), the 16 h milled sample of CaF_2 before (b) and after thermal treatment in the thermobalance (c).

due to the release of water adsorbed at the surfaces as could be shown by the ion current curve for the mass number m/z:18 in a coupled TA-MS measurement (not shown here). The mass loss of the mechanochemically synthesized samples is with 4.84% distinctly larger. Here, beside a release of water a release of CO_2 (m/z: 44) could be observed originating from traces of CO_3^{2-} in the sample. Although the thermal treatment (TG-DTA) was performed up to 800 °C, no exothermal recrystallization peak could be registered in *all* samples studied here. The only observed small effects are unspecific drifts of the DTA curves. Obviously, possible thermal effects at the reorganization of the samples cannot be proven unambiguously under the mentioned conditions.

3.3. TEM

Particles of unmilled CaF_2 have a size of up to several micrometers present as cubes or small blocs. The habit of the particles along with the electron diffraction pattern reflect the cubic crystal structure (not shown here). Sixteen hours of milling using five balls led to a strong reduction of particle size. Spherical particles as well as jagged particles with edges issue now with a diameter between 20 and 60 nm (cf. Fig. 5). For some particles the size goes down even to 2 nm and agglomeration is observed. As the enlargement given in Fig. 5 demonstrates, some of the grains show the start of amorphization in their grain boundaries. Other, non-spherical grains, however, are crystalline, even in their surface area.

In the sample milled for 16 h with ten balls the diminishing of the particle size further continues (see Fig. 6). There exist particles with diameters between 10 and 50 nm, partly separated and partly agglomerated. In addition, a fraction of very small particles occurs (Ø: 2–3 nm, see Fig. 6). Again, only the grain boundaries of

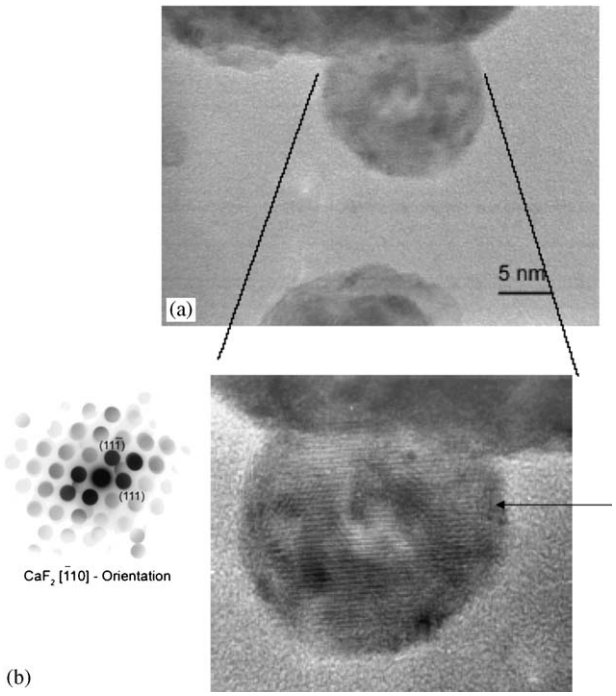

Fig. 5. TEM micrograph (a) of CaF_2 milled for 16 h (5 balls); the blow-up (see arrow) shows the beginning amorphization on the surface of a spherical particle. In the volume the particle is crystalline, lattice fringes can be seen and the electron diffraction pattern (b) of the particle shows the reflections of CaF_2.

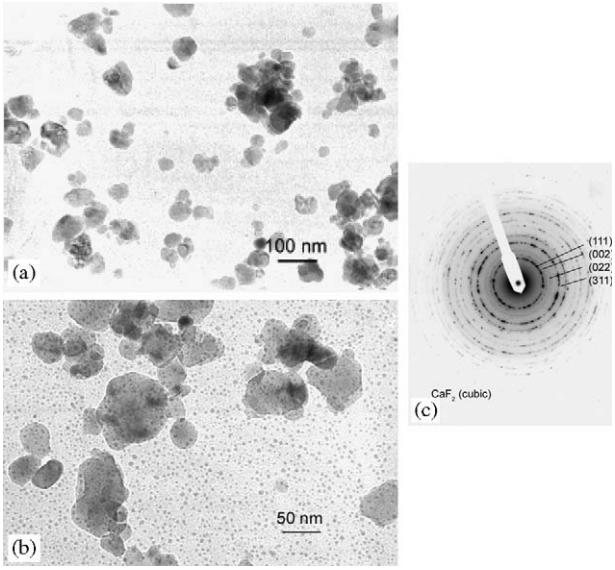

Fig. 6. TEM micrograph of CaF_2 milled for 16 h with 10 balls. Figures (a) (scale: 100 nm) and (b) (scale: 50 nm) give an overview on different particle sizes of the sample. The agglomerates of the particles show electron diffraction patterns (c) of CaF_2.

spherical particles seem to be amorphous. On the other hand, jagged particles possess *still* crystalline grain boundaries. A complete amorphization of grains could *not* be established. The cubic crystal phase of CaF_2 was identified in all, even in the small, particles. All crystallites give the typical electron diffraction patterns of CaF_2.

3.4. ^{19}F MAS NMR

^{19}F MAS NMR spectra taken with a spinning frequency of 30 kHz are given in Fig. 1b for the unmilled and the 16 h milled commercial sample. In all samples only one species could be identified with an isotropic chemical shift of $\delta_{iso} = -108.6$ ppm, typical für ^{19}F in CaF_2 [37,38]. With increasing milling time the line widths of the ^{19}F resonances enlarge and consequently the amplitudes decrease [39]. As already stated for XRD findings, the relative largest effect is also observed after 4 h of milling. After that nearly no changes occur concerning the line width. This result could be confirmed by simulating the spectra [34] with the calculated values summarized in Table 1. For longer milling times (4 h, 10 balls; or $\geqslant$8 h) it becomes more and more difficult to fit the spectra with the parameters of only one species. A small fraction of a slightly more deshielded ^{19}F-species has to be considered (see Table 1). This proportion increases slightly with increasing milling time.

In agreement with findings of XRD (cf. Fig. 4), thermal annealing at 800 °C of the 16 h milled sample results in an ^{19}F MAS NMR spectrum quite similar to the unmilled CaF_2 (not shown here). The ^{19}F MAS NMR spectra of the mechanochemically synthesized CaF_2 samples are almost the same as those of the 16 h milled samples and can be calculated with the same parameters as given in Table 1.

Table 1
Calculated values of the isotropic chemical shifts (δ_i), line widths (ΔB), and integral portions (I) of ^{19}F-resonances of milled CaF_2 samples[a]

CaF_2 samples	δ_i (ppm)	ΔB (kHz)[b]	I (%)
Unmilled	−108.6	0.99	97.3
	−106.0	0.80	2.7
4 h/5 balls	−108.9	1.37	96.2
	−105.9	0.92	3.8
4 h/10 balls	−108.7	1.41	95.2
	−105.2	1.45	4.8
8 h/5 balls	−108.9	1.37	94.2
	−106.2	1.42	5.8
16 h/5 balls	−108.7	1.38	91.7
	−105.5	1.71	8.3
16 h/10 balls	−108.7	1.38	91.7
	−105.5	1.71	8.3

[a]Simulated with the DMFIT program [34] every spectrum was calculated including two ^{19}F resonance absorptions; ^{19}F MAS NMR spectra were taken at $\nu_{rot} = 30$ kHz.
[b]A Gaussian line shape was used for the resonance at −105.5 ppm; 0.31% Gaussian character (0.69% Lorentz character) was taken for the line at −108.6 ppm.

Beside the line width of the ^{19}F resonance and its changes in dependence on time and impact of mechanical milling, the ^{19}F spin lattice relaxation times T_1 allow a sensitive indication regarding changes of the state of order of the matrices. The T_1 values as determined for the main signal at −108.6 ppm by the inversion recovery technique are listed in Table 2. Beginning with a T_1 value of 91.2 s for the unmilled sample, the T_1 times drop exponentially with increasing milling time and impact. The value obtained for the 16 h milled sample (10 balls) amounts to only 3.7% of the original T_1 time of the unmilled sample.

It is remarkable that the spin lattice relaxation times of the two mechanochemically synthesized CaF_2 samples are with 10.7 and 4.1 s comparable to those of the commercial sample milled for 16 h (see Table 2).

3.5. ^{1}H MAS NMR

Although the content of adsorbed water in the CaF_2 samples is very low (cf. DTA results), ^{1}H MAS NMR spectra allowed to assign different ^{1}H species.

The measured ^{1}H MAS NMR spectra of the studied samples obtained under identical conditions are summarized in Fig. 7. The use of a spinning frequency of 30 kHz results in high-resolved ^{1}H NMR spectra with only one pair of spinning sidebands with an intensity of less than 3% of the whole intensity of the corresponding spectra. Therefore, only the central parts of the three spectra are shown.

The ^{1}H MAS NMR spectrum of the unmilled CaF_2 sample (Fig. 7a) consists of two sharp separated signals at

Table 2
Spin lattice relaxation times T_1 of the ^{19}F resonance in CaF_2 (−108.6 ppm) determined in dependence on time and impact of mechanical milling

Matrix	T_1 (s)
Commercial CaF_2 (Riedel) Unmilled	91.2
CaF_2 4 h milled, 5 balls	22.7
CaF_2 16 h milled, 5 balls	7.5
CaF_2 4 h milled, 10 balls	3.9
CaF_2 16 h milled, 10 balls	3.4
Mechanochemically synthesized CaF_2 5 h milled	10.7
10 h milled	4.1

1.1 and 5.4 ppm as well as a broad shoulder at 12 ppm. The signal at 1.1 ppm is probably attributed to isolated hydroxyl groups at the surface of the CaF_2 crystals. For protons in $Ca(OH)_2$ chemical shifts of 1.2 ppm have been measured [40]. But also weak hydrogen bridged F···H–O species, as described by Jesinowski and Eckert [41] for protons in fluorohydroxyapatites show a chemical shift value at 1.2 ppm. The signal at 5.4 ppm can be attributed to surface adsorbed water. In proton containing oxides a signal at 12 ppm indicates the existence of strongly hydrogen bonded protons [40,42]. Since chemical shift values of 0.6 and −0.5 ppm have been determined for CaH_2 (not shown here), a simple replacement of F^- ions by H^- ions in the sample of CaF_2 and the formation of local calcium hydride substructures could not be indicated. Therefore, in the studied sample of commercial CaF_2 the observed strongly hydrogen bonded protons (12 ppm) are assumed to be located on lattice defects of the sample. After γ-irradiation of the unmilled sample, especially the shoulder at 12.0 ppm disappears (see Fig. 7b).

The ^1H MAS NMR spectrum of the 16 h milled CaF_2 sample (Fig. 7c) shows a more intensive NMR signal compared with that of the unmilled sample. This observation indicates an uptake of protons during or after the milling process. As in the case of the unmilled sample small signals for strongly hydrogen bonded protons at 12 ppm and for isolated hydroxyl groups at the surface of the crystals at 1.1 ppm are detectable. The maximum of the signal is shifted to 4.6 ppm and an additional signal at 7.0 ppm is observed. The signal at 4.6 ppm can be attributed to physisorbed water at the enlarged surface of the milled sample. This interpretation is supported by the measurement of a milled CaF_2 sample that has been dried for 24 h at 373 K under vacuum conditions. For this specially prepared sample a strong reduction of the signal at 4.6 ppm was observed (not shown here). The signal at 7.0 ppm is assigned to protons in hydrate-like phases. While in oxide hydrates the chemical shift for protons in crystal water occupy a range from 4 ppm till to 6 ppm [40,42] our own studies on fluoride hydrates have shown chemical shift values up to 8 ppm (not shown here). The ^1H MAS NMR spectrum of the mechanochemically synthesized CaF_2 sample (Fig. 7d) is very similar to that of the corresponding spectrum of the 16 h milled CaF_2 sample but the intensity is higher. This is due to the fact that during the reaction water has been formed. A shoulder at 12 ppm is not detectable and the content of protons in hydrate-like phases increases.

3.6. EPR

Atomic hydrogen represents an electron spin probe of at least three advantages: it can only be trapped (i) if suitable traps (high-symmetric cages) are accessible and give characteristic hyperfine pattern for a doubtless assignment

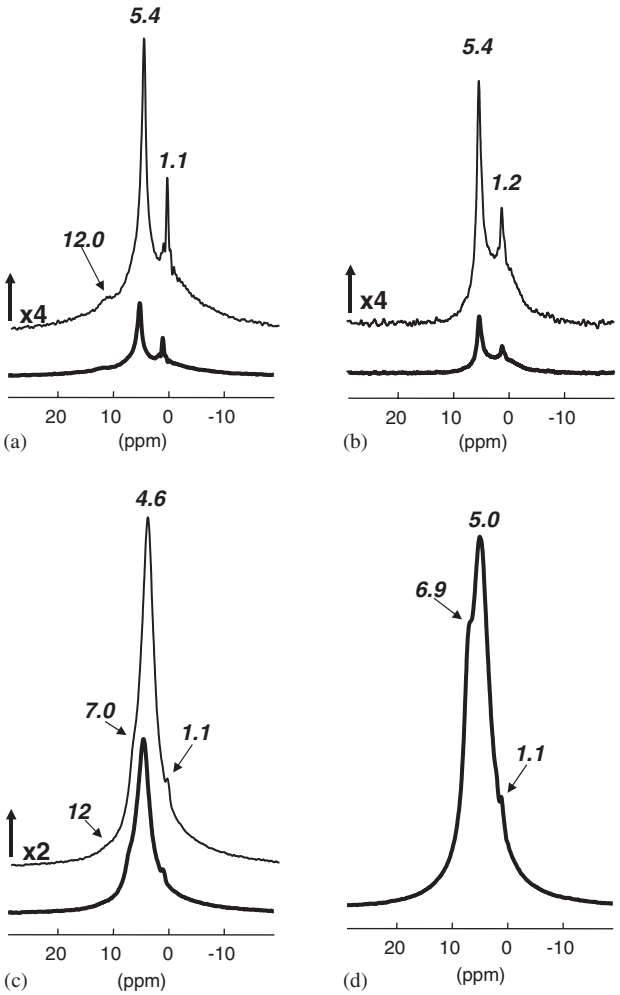

Fig. 7. ^1H MAS NMR spectra of: (a) unmilled CaF_2; (b) unmilled CaF_2 after γ-irradiation (100 kGy); (c) a 16 h (5 balls) milled CaF_2; and (d) a mechanochemically synthesized sample from $CaCO_3$ and NH_4F(10 h milling) (2.5 mm rotor, $\nu_{rot} = 30$ kHz).

of the ESR signals; (ii) if $H^{\bullet}$ precursors are present in the samples or can be provided externally; and (iii) if the generated $H^{\bullet}$ atoms own the adequate energy to enter the cage. Interactions with lattice or electronic defects or other scattering processes caused by the degrees of freedom in the matrix therefore change the energy of the $H^{\bullet}$ atoms and the yield of trapped atoms will be diminished. Depending on the degrees of freedom of the matrix, the spin relaxation behaviour is changed in a characteristic manner.

It is well known that atomic hydrogen $H^{\bullet}$ can be trapped in single crystals [24–27] as well as in powders of CaF_2 [28–30] at room temperature. In comparison to $H^{\bullet}$ in AlF_3 [29,43–45], the atomic hydrogen $H^{\bullet}$ stabilized in CaF_2 powders has a different behaviour concerning the temperature dependence of the hyperfine coupling constant (hfcc) [29], concerning thermal decay reactions and the saturation behaviour of its EPR signal [30]. A detailed study will be subject of a separate paper [46].

The untreated commercial CaF_2 charge used for the present investigations bears good prerequisites for $H^{\bullet}$ trapping. Therefore, the changes caused by the milling process can easily be watched by the amplitudes of the corresponding ESR signals as a function of the microwave power applied.

In the mechanochemically synthesized CaF_2 samples a trapping of $H^{\bullet}$ atoms at room temperature could not be evidenced.

Surprisingly, the milled commercial CaF_2 samples investigated in the present contribution have the ability to trap $H^{\bullet}$ produced by γ-irradiation (100 kGy) at 298 K. The $H^{\bullet}$ signals could be recorded at 292 K and 2 mW (100 kHz modulation frequency) as regular first derivatives of the EPR signal. Moreover, different $H^{\bullet}$ sites could be identified after milling (see Fig. 8, inset). The low-field signals of the X-band EPR spectra of both the unmilled and 16 h milled CaF_2 powder samples are given in Fig. 8. Whereas the unmilled sample hosts one detectable species of $H^{\bullet}$ with an hfcc of $A_{hfc} = 1403.8$ MHz (amplitude A_1), with increasing milling time a second species with a larger hfcc ($A_{hfc} = 1459.2$ MHz) [29] distinctly appears in addition (amplitude A_2). The mass normalized amplitude A_1 of the initial species decreases exponentially with increasing milling time. At the same time the amplitude A_2 of the second $H^{\bullet}$ species increases slightly in relation to the first one (see Fig. 9). The integral intensity however of all trapped $H^{\bullet}$ atoms decreases with increasing milling time.

At 4.2 K and a modulation frequency of 100 kHz (2 mW microwave power) the $H^{\bullet}$ signals of the unmilled sample appear with an absorption-like shape because of the admixture of dispersion contributions. Here, the product T_1T_2 is too large to follow the 100 kHz effect modulation due to absence of effective fluctuations in the system at this temperature. Therefore, at 4.2 K a modulation frequency of 1 kHz was applied to determine the saturation curves of trapped $H^{\bullet}$ atoms in both unmilled and milled CaF_2 samples (cf. Fig. 10). Whereas the unmilled sample gives the typical saturation curves of trapped $H^{\bullet}$ atoms [47], for

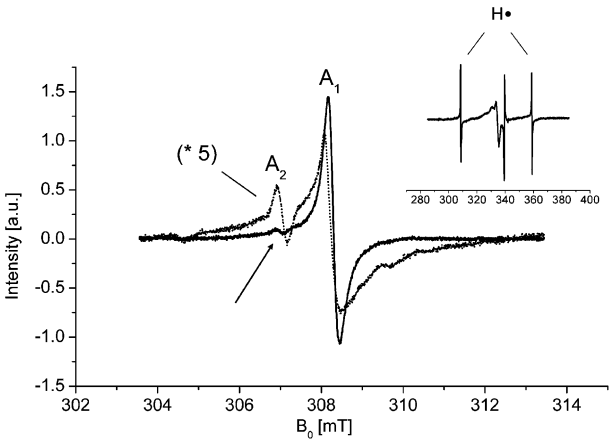

Fig. 8. X-band EPR spectra (low-field signals, 293 K) of $H^{\bullet}$ in CaF_2 recorded after γ-irradiation (100 kGy) of unmilled CaF_2 (___, amplitude A_1) and 16 h (5 balls) milled CaF_2 (…, amplitudes A_2). The signals of the two species are mass normalized. Inset: X-band EPR spectrum of unmilled CaF_2.

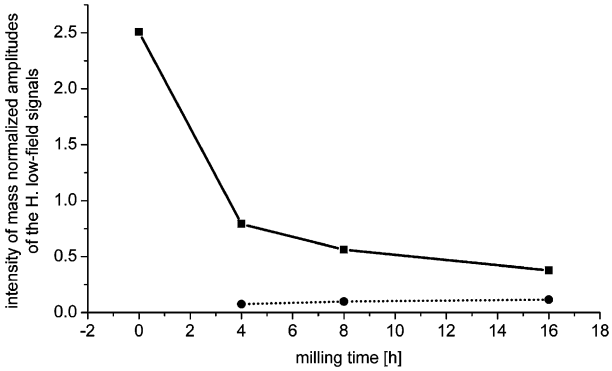

Fig. 9. Mass normalized amplitudes A_1 (■)and A_2(●) of the two low-field signals of $H^{\bullet}$ in CaF_2 in dependence on milling time.

the mechanically treated samples the saturation behaviour has the typical shape of inhomogeneous broadened lines. The latter results due to statistical distributions of distortions of trapping positions as a consequence of mechanically induced small matrix perturbations.

Inspecting the EPR spectra of non-irradiated samples using a large B_0-scale up to 500 mT the following can be stated:

After 4 h of milling the broad spectral contributions of the low-field part of the X-band EPR spectra ($0 < B_0 < 250$ mT) indicates the formation of dangling bonds and defect pairs in the sample (not shown here). At longer milling times the spectral pattern in this region is changed by aggregation, transformation and recombination processes of the unsaturated bonds and defect pairs.

Finally, it should be mentioned that the milled CaF_2 samples thermally treated up to 800 °C did not allow the trapping of $H^{\bullet}$ atoms due to the reduced amount of precursors and the number of accessible intact cage-like structural elements.

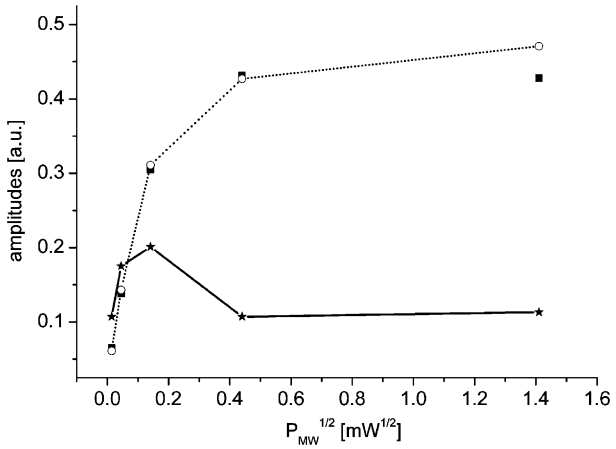

Fig. 10. Amplitude of the low-field X-band EPR signal of $H^{\bullet}$ in CaF_2 in dependence on the microwave power, taken at 4.2 K with a modulation frequency of 1 kHz; ■ CaF_2, 16 h milled (10 balls); ● CaF_2, 4 h milled (10 balls); *unmilled CaF_2.

4. Discussion

The mechanochemical synthesis of CaF_2 from $CaCO_3$ and NH_4F performed for the first time in this study was successful with CaF_2 as the only solid product. Nearly all properties of this CaF_2 (^{19}F and ^{1}H resonances, ^{19}F-T_1 relaxation times, XRD reflections, vide infra) are comparable to those of the long time milled commercial sample. It means the result should be also in this case a *nanocrystalline* calcium fluoride. However, as deviation from results obtained for the commercial sample, atomic hydrogen could not be trapped in the synthesized CaF_2 powders although a sufficient concentration of possible H-precursors is present in the sample (see Fig. 7d). Therefore, the trapping of $H^{\bullet}$ atoms in such matrices can be regarded as an important discriminative criterion concerning the real structure of a mechanically treated sample.

As it could be established by XRD and TEM methods, mechanical milling of commercial CaF_2 leads as expected to a remarkable reduction of the particle size. The extent of reduction depends both on the duration of mechanical treatment and on the strength of the impact (five or 10 balls). Particles ranging from 2 nm to 3 nm can be observed (Fig. 6). It means that a certain amount of particles appear with only 4–6-fold sizes of an unit cell in CaF_2 (cf. Fig. 1a). Unexpectedly, even after the strongest mechanical impact applied here the samples are *nanocrystalline*. A noticeable amorphous part could not be found. The latter was additionally confirmed with DTA measurements by the absence of a recrystallization peak. A weak beginning amorphization could be observed only at the surfaces of some spherical particles.

These results are in agreement with the observed XRD amplitude ratios as described in the results part. It is well known that the cleavage face of CaF_2 is the (1 1 1) plane. It means the symmetry of the crystallites is conserved at grinding along this plane and cleavage is one of the dominant processes induced mechanically. Consequently, the corresponding reflection in the X-ray diffractogram is less effected than the (0 2 2) reflection at milling. A stronger perturbation of the symmetry and therewith of the lattice periodicity takes place in the [0 2 2] direction. After thermal treatment, the restored XRD amplitude ratio $A_{1\,1\,1}/A_{0\,2\,2}$ together with the re-established ^{19}F MAS NMR spectrum, support the idea of a healing up of grains, meaning a reorganization whereby the lattice periodicity is restored.

Bearing these results in mind, line broadening effects of ^{19}F resonances and the decrease of the spin lattice relaxation times T_1 with increasing milling time are then a consequence of the reduced particle size and the accompanying very small deviations from the cubic symmetry in the bulk of the nanoparticles.

A quantitative consideration reveals that the changes of the dynamic parameters of the magnetic resonance do not correlate with the issue of the small amorphous proportion in some grain boundaries. Therefore, both the line widths of the main ^{19}F resonances and the T_1 relaxation times obtained for this transition appear to be sensitive tools to indicate actually the increasing surface to bulk ratio in the samples occurring with increasing milling time. They indicate also very small deviations from the equilibrium geometric and electronic structure of the matrix. The systematic lowering of the ^{19}F spin lattice relaxation time T_1 with increasing milling time represents a result of the rising number of lattice defects. The electronic and geometric defects open additional relaxation channels. The formation of electronic defects, especially in the form of anion disorder and the resulting ionic conductivity is in general known for CaF_2.

In contrast, the issue of a small proportion of an additional fluorine species (up to 8%, $\delta_{iso} = -105.5$ ppm, broad lines, see Table 1) with a higher distorted environment correlates very well with the beginning amorphization in spherical grain boundaries (see TEM results). The ^{1}H signal at 7 ppm of these samples (Figs. 7c and d) was assigned to protons in hydrate-like regions and supports the idea of the appearance of those species probably in the amorphous surface regions of the spherical particles.

As the ^{1}H MAS NMR spectra (Fig. 7) show, there are different ^{1}H species in the samples which could not only be able to yield trapped $H^{\bullet}$ atoms, detectable by EPR spectroscopy (see Ref. [45]), but also act as important indicators for the chemical composition and dynamics of the surface region. MAS NMR measurements after γ-irradiation of the unmilled sample support the idea that mainly strongly hydrogen bonded protons (signal at 12 ppm) serve as precursors for atomic hydrogen. This signal is distinctly affected by γ-irradiation (for comparison see Figs. 7a and b).

As previous investigations evidenced, $H^{\bullet}$ trapping at ambient temperatures after γ-irradiation needs high symmetric cages of certain size [43,44].

Due to strongly decreased particle sizes and the accompanying microstructural changes by milling, the number of such sites is reduced. This circumstance could explain the exponential decay behaviour of the amplitude A_1 of the low-field signal of $H^\bullet$ (Figs. 8 and 9). It is interesting to note that there is a correspondence of the decay function to the decay function of ^{19}F T_1 relaxation times.

The milling process is just responsible for a reduction of the number of symmetric trapping sites for atomic $H^\bullet$. In addition to this phenomenon, one has to take into account that the mechanically activated solid bears a lot of scatter and recombination centres (e.g., traces of defects and defect pairs) which will diminish the number of $H^\bullet$ atoms suitable for trapping. Similar effects have to take into account in samples prepared by mechanosynthesis. Here, the residues of starting materials (like CO_3^{2-} as evidenced by CO_2 in TA-MS measurements) can disturb the structure of the matrix. They can also act as diffraction and reaction centres for the $H^\bullet$ atoms.

As in the case of nuclear spins, mechanically induced activations of the matrix essentially contribute to a minor saturation tendency of the $H^\bullet$ spin system by an increase of suitable fluctuations of the matrix even at low temperature. This view allows also a simple explanation for the issue of the observed second $H^\bullet$ signal with the larger hfcc after mechanical activation. Obviously, this signal is already present in the unmilled and γ-irradiated CaF_2 (see arrow in Fig. 8). However, applying low microwave powers and a 100 kHz modulation frequency broadened it due to the passage effect. The larger hyperfine coupling constant, the smaller line width as well as the pronounced saturation tendency imply a weaker interaction with the environment and favours a stabilization on interstitial positions, symmetrically surrounded by eight fluorine atoms.

5. Conclusion

Based on the methods applied in this study the following findings of novelty can be summarized:

In contrast to many oxide compounds, e.g., Refs. [48,49], milling of CaF_2 powders under the conditions applied here does not lead to a noticeable amorphization of the samples. After milling of commercial CaF_2, nanocrystalline CaF_2 is formed with a very low amorphous content in the surfaces of the particles. Surprisingly, the mechanochemically prepared sample from $CaCO_3$ and NH_4F leads to a nanocrystalline sample too.

Even the application of larger mechanical impacts (vibration mill, use of diamond as milling enhancer) resulted in the same observations.

Most of the applied methods (TEM, XRD, ^{19}F chemical shift in MAS NMR) show unambiguously the influence of the milling process and allow to compare properties of crystalline and nanocrystalline CaF_2. The perturbation of the structure as observed with solid state magnetic resonance methods as well as XRD and TEM measurements together with the absence of DTA effects is not very large and almost reversible. Obviously, the cleavage of the CaF_2 crystallites present or chemically formed in the sample is the dominating process at the milling of such samples.

However, the very small deviations between mechanically treated and mechanochemically synthesized samples are only hardly detected. Even the T_1 relaxation times of the ^{19}F spin probes at a fixed temperature of 293 K can only be heavily distinguished for CaF_2 prepared in the two ways.

The best diagnostic mean giving clear differences is the extend of $H^\bullet$ trapping and its microwave saturation behaviour.

Relevant macroscopic properties of CaF_2 like the complete cleavability parallel to the (1 1 1) plane formed by one kind of ions, the comparably low melting point of 1403 °C and not at least the formation of lattice defects after thermal treatments or exposure to ionizing radiation can be brought in relation to spin-relaxation behaviour of the mechanically treated CaF_2 matrices.

Based on the specifics of the metal-fluoride bonds, the structural relaxation processes of solid fluorides are quite different compared to those obtained by oxides: e.g., on mechanical milling of corundum (α-Al_2O_3) [50].

Acknowledgments

Prof. Dr. E. Kemnitz (Humboldt University of Berlin) is kindly acknowledged for giving the access to the XRD equipment, Dr. A. Zehl (Humboldt University of Berlin) for some EPR measurements and Dr. E. Janata (Hahn-Meitner Institute of Berlin) for performing γ-irradiations. Dr. S. Steuernagel (Bruker Biospin) is kindly acknowledged for giving access to the pulse program to suppress ^{19}F and ^{1}H probehead signals. R. Köppen and O. Kaczmarek are acknowledged for the mechanosynthesis of CaF_2.

References

[1] Proceedings of the International Conference on Mechanical Milling (INCOME) 2003, 7–11 September 2003, Braunschweig, Germany.
[2] V.V. Boldyrev, Reactivity of Solids: Past, Present and Future, Blackwell Science: Oxford, 1996.
[3] E. Gaffet, F. Bernard, J.-C. Niepce, F. Charlot, C. Gras, G. Le Caer, J.L. Guichard, P. Delcroix, A. Mocellin, O. Tillement, J. Mater. Chem. 9 (1999) 305–314.
[4] E. Gaffet, D. Michel, L. Mazerolles, P. Berthet, Mater. Sci. Forum 235–238 (1997) 103–108.
[5] D. Michel, L. Mazerolles, P. Berthet, E. Gaffet, Eur. J. Solid State Inorg. Chem. 32 (1995) 673–682.
[6] E. Avakumov, M. Senna, N. Kosova, Soft Mechanochemical Synthesis: A Basis for New Chemical Technologies, Kluwer Academic Publishers, Boston, 2001.
[7] E. Kemnitz, U. Groß, S. Rüdiger, C.S. Shekar, Angew. Chem. 115 (2003) 4383–4386.
[8] S. Fujihara, S. Ono, Y. Kishiki, M. Tada, T. Kimura, J. Fluorine Chem. 105 (2000) 65–70.

[9] S. Rüdiger, U. Groß, M. Feist, H. Prescott, C.S. Shekar, S.I. Troyanov, E. Kemnitz, J. Mater. Chem. 15 (2005) 588–597.
[10] J.K. Murthy, U. Groß, S. Rüdiger, E. Ünveren, E. Kemnitz, J. Fluorine Chem. 125 (2004) 937–949.
[11] J. Lee, Q. Zhang, F. Saito, Chem. Lett. (2001) 700–701.
[12] J. Lu, Q. Zhang, F. Saito, Chem. Lett. (2002) 1176–1177.
[13] J. Lee, Q. Zhang, F. Saito, J. Am. Ceram. Soc. 84 (2001) 863–865.
[14] M. Kumar, S.S. Sekhon, J. Phys. D: Appl. Phys. 34 (2001) 2995–3002.
[15] M. Kumar, K. Yamada, T. Okuda, S.S. Sekhon, Phys. Stat. Sol. (b) 239 (2003) 432–438.
[16] M. Uno, M. Onitsuka, Y. Ito, S. Yoshikado, Solid State Ionics 176 (2005) 2493–2498.
[17] E. Reguera, J. Fernandez-Bertran, A. Paneque, H. Yee-Madeira, Spectrosc. Lett. 37 (2004) 191–199.
[18] Y. Wu, Y. Zhang, G. Pezotti, J. Guo, Mater. Lett. 52 (2002) 366–369.
[19] M. Bervas, F. Badway, L.C. Klein, G.G. Amatucci, Electrochem. Solid State Lett. 8 (4) (2005) A179–A183.
[20] B. Bureau, H. Guérault, G. Silly, J.Y. Buzaré, J.M. Grenéche, J. Phys.: Condens. Matter 11 (1999) L423–L431.
[21] H. Guérault, B. Bureau, G. Silly, J.Y. Buzaré, J.M. Grenéche, J. Non-Cryst. Solids 287 (2001) 65–69.
[22] M.A.C. Wevers, J.C. Schön, M. Jansen, J. Phys.: Condens. Matter 11 (1999) 6487–6499.
[23] M.A.C. Wevers, J.C. Schön, M. Jansen, J. Solid State Chem. 136 (1998) 233–246.
[24] J.L. Hall, R.T. Schumacher, Phys. Rev. 127 (6) (1962) 1892–1912.
[25] S.G. Sligar, H. Blum, Phys. Rev. B 3 (11) (1971) 3587–3592.
[26] R.G. Bessent, W. Hayes, J.W. Hodby, P.H.S. Smith, Proc. R. Soc. A 309 (1969) 69–90.
[27] F.J. Adrian, J. Chem. Phys. 32 (4) (1960) 972–981.
[28] B. Welber, Phys. Rev. A 136 (1964) 1408–1412.
[29] G. Scholz, Spin probes in solids with coexisting crystalline and non-crystalline regions—Aspects of local structure in fluorides and oxides of aluminium. Habilitation Thesis, Humboldt University of Berlin, 2004.
[30] M. Ahrens, Diploma Thesis, Humboldt University of Berlin, 2004.
[31] I. Nikcevic, V. Jokanovic, M. Mitric, Z. Nedic, D. Makovec, D. Uskokovic, J. Solid State Chem. 177 (1994) 2565–2574.
[32] M. Mehring, V.A. Weberruß, Object-Oriented Magnetic Resonance, Academic Press, New York, 2001.
[33] D.G. Cory, W.M. Ritchey, J. Magn. Reson. 80 (1988) 128–132.
[34] D. Massiot, F. Fayon, M. Capron, I. King, S. Le Calvé, B. Alonso, J.O. Durand, B. Bujoli, Z. Gan, G. Hoatson, Magn. Reson. Chem. 40 (2002) 70–76.
[35] J.F. Brice, A. Courtois, J. Aubry, J. Solid State Chem. 24 (1978) 381.
[36] J. Bergmann, R. Kleeberg, T. Taut, A. Haase, Adv. X-ray Anal. (1997) 40.
[37] J.M. Miller, Prog. Nucl. Magn. Reson. Spectrosc. 28 (1996) 255–281.
[38] R.K. Harris, P. Jackson, Chem. Rev. 91 (1991) 1427–1440.
[39] To observe this effect quantitatively, the respective relaxation times have to be included for each sample in the recycling delay ($5T_1$).
[40] D. Heidemann, in: A. Colombet, A.-R. Grimmer (Eds.), Application of NMR Spectroscopy to Cement Science, Gordon & Breach, London, 1993, pp. 77–102.
[41] J.P. Yesinowski, H. Eckert, J. Am. Chem. Soc. 109 (1987) 6274–6282.
[42] J.P. Yesinowski, H. Eckert, G.R. Rossmann, J. Am. Chem. Soc. (1988) 1367–1375.
[43] G. Scholz, R. Stösser, J.A. Momand, A. Zehl, J. Klein, Angew Chem. Int. Ed. 39 (14) (2000) 2516–2519.
[44] G. Scholz, R. Stösser, Phys. Chem. Chem. Phys. 4 (22) (2002) 5448–5457.
[45] R. Stösser, G. Scholz, A. Zehl, J. Klein, in: Proceedings of the 16th Colloque International on Hertzian Optics and Dielectrics, OHD 2001 Le Mans, 3–5 September 2001, pp. 69–72.
[46] R. Stösser, M. Ahrens, G. Scholz, J. Phys. Chem. 2006, in preparation.
[47] J.A. Weil, J.R. Bolton, J.E. Wertz, Electron Paramagnetic Resonance: Elementary Theory and Practical Applications, Wiley, New York, 1994.
[48] J. Xue, D. Wan, S.E. Lee, J. Wang, J. Am. Ceram. Soc. 2 (7) (1999) 1687–1692.
[49] A.A. Shubin, O.B. Lapina, E. Bosch, J. Spengler, H. Knözinger, J. Phys. Chem. B 103 (1999) 3138–3144.
[50] G. Scholz, R. Stösser, G. Silly, J.Y. Buzaré, Y. Laligant, B. Ziemer, J. Phys.: Condens. Matter 14 (2002) 2101–2117.
[51] M. Binnewies, M. Jäckel, H. Willner, G. Rayner-Canham, Allgemeine und Anorganische Chemie, Spektrum Akademischer Verlag, Heidelberg, Elsevier, GmbH München, 2004.